Geophys. J. Int. (1999) **138,** 871-878

Lithospheric structure of the Arabian Shield and Platform from complete regional waveform modelling and surface wave group velocities

Arthur J. Rodgers,' William R. Walter,' Robert J. Mellors,- Abdullah M. S. Al-Amri[3] and Yu-Shen Zhang[4]

'Lawrence Livermore National Laboratory, Geophysics and Global Security Division, PO Box 808, Livermore, CA 94551-9900, USA. E-mail: rodgers7@llnl.gov

'San Diego State University, Department of Geological Sciences, San Diego, CA, USA

'King Saud University, Geophysical Observatory, Riyadh, Kingdom of Saudi Arabia

° University of California, Santa Cruz, Institute of Tectonics, Santa Cruz, CA, USA

Accepted 1999 May 10. Received 1999 April 19; in original form 1998 November 13

SUMMARY

Regional seismic waveforms reveal significant differences in the structure of the Arabian Shield and the Arabian Platform. We estimate lithospheric velocity structure by modelling regional waveforms recorded by the 1995-1997 Saudi Arabian Temporary Broadband Deployment using a grid search scheme. We employ a new method whereby we narrow the waveform modelling grid search by first fitting the fundamental mode Love and Rayleigh wave group velocities. The group velocities constrain the average crustal thickness and velocities as well as the crustal velocity gradients. Because the group velocity fitting is computationally much faster than the synthetic seismogram calculation this method allows us to determine good average starting models quickly. Waveform fits of the *Jon* and Sn body wave arrivals constrain the mantle velocities. The resulting lithospheric structures indicate that the Arabian Platform has an average crustal thickness of 40 km, with relatively low crustal velocities (average crustal P- and S-wave velocities of 6.07 and 3.50 km s^{-1}, respectively) without a strong velocity gradient. The Moho is shallower (36 km) and crustal velocities are 6 per cent higher (with a velocity increase with depth) for the Arabian Shield. Fast crustal velocities of the Arabian Shield result from a predominantly mafic composition in the lower crust. Lower velocities in the Arabian Platform crust indicate a bulk felsic composition, consistent with orogenesis of this former active margin. P- and S-wave velocities immediately below the Moho are slower in the Arabian Shield than in the Arabian Platform (7.9 and 4.30 km s^{-1}, and 8.10 and 4.55 km s^{-1}, respectively). This indicates that the Poisson's ratios for the uppermost mantle of the Arabian Shield and Platform are 0.29 and 0.27, respectively. The lower mantle velocities and higher Poisson's ratio beneath the Arabian Shield probably arise from a partially molten mantle associated with Red Sea spreading and continental volcanism, although we cannot constrain the lateral extent of a zone of partially molten mantle.

Key words: crustal structure, lithosphere, surface waves, waveform analysis.

INTRODUCTION

The Arabian Peninsula is composed of the (western) Arabian Shield and the (eastern) Arabian Platform (Fig. 1). Several distinct terranes make up the Shield, with the eastern terranes having continental affinity and the western terranes having island arc affinity (Stoeser & Camp 1985). Unlike most continental shield regions, the Arabian Shield contains areas of recent volcanism. Locations of Neogene-Quaternary basalt cover, related to recent continental volcanic activity, are shown in Fig. 1. Camp & Roobol (1992) analysed rocks from these sites and found evidence for two episodes of volcanism. They concluded that the more recent phase of volcanic activity (12 Ma to present) is related to active mantle upwelling contemporaneous with the uplift of western Arabia. The Arabian Platform shows no volcanic activity. Proterozoic basement is

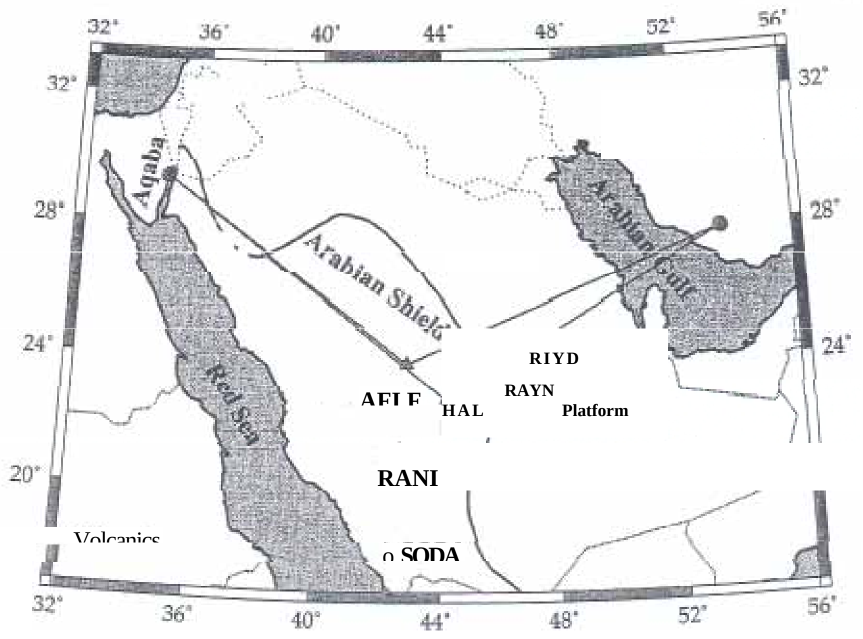

Figure 1. Map of the Arabian Peninsula showing the locations of the earthquakes (circles), stations (triangles) and paths (grey lines) considered. The heavy black line marks the approximate boundary between the sediment cover of the Arabian Platform and the exposed basement of the Arabian Shield. The grey shading indicates Neogene-Quaternary basalt cover.

exposed in the Shield; however, the Platform is covered by Phanerozoic sediments which gradually thicken (west-to-east) to nearly 10 km in the Mesopotamian Foredeep and Arabian Gulf (Seber *et al.* 1997). Eastward oceanic subduction and collision of continental terranes led to orogenesis along the western margin of the Arabian Platform in Late Proterozoic times (Stoeser & Camp 1985). The Arabian Gulf is underlain by continental crust which is currently colliding with the Eurasian Plate along the Zagros Thrust.

A seismic refraction profile conducted in the Arabian Shield (Gettings *et al.* 1986) is roughly coincident with the temporary broadband stations SODA, RANT, HALM, RAYN and RIYD (Fig. 1). Data from these stations revealed a 40-km thick crust in the central shield with average velocities of 6.3 km s^{-1} for the upper crust and 7.0 km s^{-1} for the lower crust and a midcrustal reflector at about 20 km depth (Gettings *et al.* 1986). That study also reported that the crust rapidly thins near the Red Sea. An interesting observation is that the topography is higher on average in the western Arabian Shield than in central Arabia, despite the inferred thinner crust. Al-Amri (1998, 1999) modelled P-wave spectra to infer crustal structure near the seismic observatory in Riyadh (a long-period analogue station near RIYD, Fig. 1). He reported fast crustal velocities, consistent with the refraction results. Regional surface wave investigations of the Arabian Peninsula revealed variations in shear wave velocity and attenuation structure. Seber & Mitchell (1992) modelled short-period (5-30 s) fundamental mode Love and Rayleigh wave spectra to estimate shear wave velocity and attenuation of the upper crust. They concluded that Q_5 in the upper crust is generally low throughout Arabia, with values of 60 for western Arabia, 100-150 for central Arabia and 65-85 for eastern Arabia. Mokhtar & Al-Saeed (1994) inverted Love and Rayleigh wave group velocity curves observed at RIYD to estimate shear wave velocity structure for paths from the Red Sea, Gulf of Aden and Zagros. They found that paths from the Red Sea to RYD, which primarily sample the Arabian Shield, are faster than paths from the Zagros and Gulf of Aden, which sample the Arabian Platform.

In this article, we present analysis of regional waveforms recorded by the 1995-1997 Saudi Arabian Broadband Deployment. From these data, we infer pure-path velocity structures for the Arabian Shield and Arabian Platform. We estimate velocity models by fitting the observed regional waveforms. We use a new method to expedite the waveform modelling grid search by first modelling the observed surface wave group velocities. The resulting lithospheric velocity models reveal significant structural differences between the shield and platform paths. The velocity structures we report for these regions provide new insights into the structure and composition of the Arabian Peninsula.

DATA

Between November 1995 and March 1997, nine temporary broadband three-component seismic stations were deployed across central Saudi Arabia (Fig. 1-we show only the six stations that had high-quality data for the events studied). The stations were located primarily on the Arabian Shield. Studies using these data report significant differences in the character of the western and eastern Arabian Peninsula from shortperiod regional phase propagation (Mellors *et al.* 1998; Walter & McNamara 1997) and surface wave group velocity dispersion (McNamara *et al.* 1997; Mokhtar *et al.* 1997; Ritzwoller & Levshin 1998; Pasyanos *et al.* 1998). Using stacked shortperiod regional seismograms, Mellors *et al.* (1998) report that mantle body wave phases (Pn and Sn) are much weaker than L_g for the Gulf of Aqaba and Syrian events observed at the Saudi Arabian temporary stations. Regional phase amplitudes for the Zagros to Saudi paths are more typical of stable continental areas. They also show that short-period L_g propagates very efficiently and that Lg velocities are faster for the Shield paths than for the Platform paths, suggesting that crustal Q and shear velocities are higher in the Shield. Estimates of lithospheric velocity and discontinuity structure beneath the temporary stations from teleseismic receiver functions are reported by Sandvol *et al.* (1998). They report that crustal thickness is about 40-45 km and that the average crustal shear wave velocity is about 3.7 km s^{-1} beneath the stations in the central Arabian Shield.

Two moderately large earthquakes recorded by the temporary stations provide excellent pure-path sampling of the Arabian Shield and the Arabian Platform (Fig. 1). Event locations and origin times are taken from the USGS Preliminary Determination of Epicentres. Double-couple focal mechanisms and scalar moments are taken from the Harvard CMT catalog. Event depths were adjusted by fitting the regional waveforms using our best-fitting velocity models. Table 1 gives the event parameters.

GROUP VELOCITY MODELLING

Surface wave group velocities in the period band 10-50 s are sensitive to lithospheric structure, especially crustal thickness and S-wave velocities. Because of the broad depth sampling of surface waves, group velocities are not uniquely related to velocity structure, but are more sensitive to the average velocitydepth profile. We modelled the observed group velocities to determine candidate velocity structures for grid search waveform modelling. The complete regional waveforms contain the body waves and the surface wave group and phase velocity information and thus have greater sensitivity to lithospheric velocity structure. Because of the non-uniqueness between surface wave group velocities and seismic velocity structure, and problems with group velocity measurement (for example measurement uncertainties, low signal-to-noise ratios, spectral .notches), estimates of velocity structure based solely on group velocity dispersion curves are probably not as accurate as those derived from waveform modelling. In fact, we found that models that fit the group velocity curves the best do not necessarily fit the observed waveforms as well as other models. Therefore, while group velocities provide some constraint on the velocity model, waveform matching provides tighter restrictions on the model because phase and amplitude information are included.

Differences between the structure of the Arabian Shield and Platform are immediately apparent from the Love and Rayleigh wave group velocity dispersion curves shown in Fig. 2. Group velocities were measured from instrument-deconvolved displacement seismograms using a multiple filter analysis code (C. Ammon, personal communication). Rayleigh and Love wave dispersion was measured on the vertical and transverse components, respectively. The curves are plotted only for periods where the surface wave amplitudes are not impacted by notches in the amplitude spectrum and/or poor signal

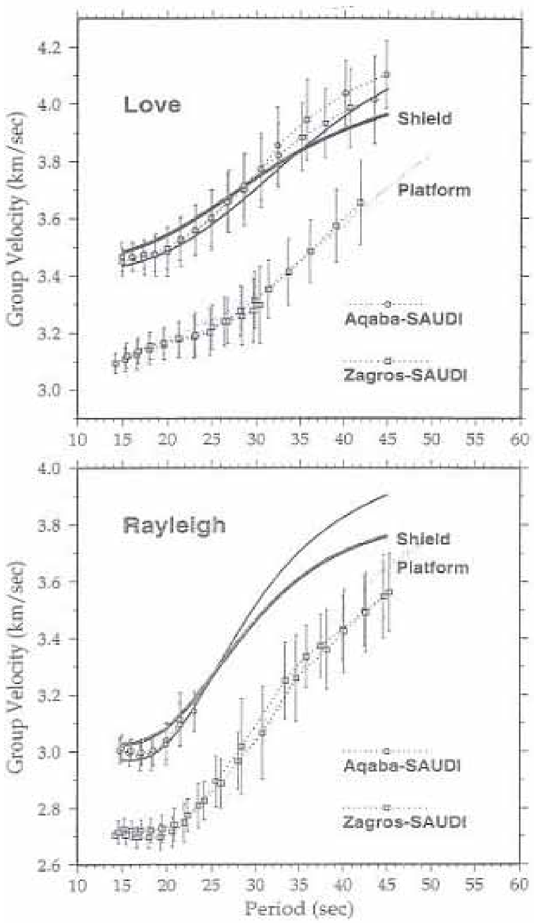

Figure 2. Love (top) and Rayleigh (bottom) wave group velocity dispersion curves and errors for the Aqaba (circles) and Zagros (squares) paths to stations AFIF and HALM. The thin lines are the group velocity curves for the models that provide the best fits to the group velocities. The thick lines are the group velocity curves for the preferred models which provide the best fit to the complete waveforms.

to-noise ratio. This is why the Rayleigh wave group velocity curve for the Aqaba to Saudi path is cut at about 23 s. Uncertainties are ad hoc and set to the 90 per cent reduction in amplitude of the frequency-time surface at each period. The

Table 1. Source parameters of events used in this study. Events are identified in Fig. 1 by their year and day of year (yy-ddd).

Event	Origin Time (GMT)	Latitude	Longitude	Depth (km)	Mb	Strike/Dip/Rake
95-327	1995 Nov. 23 (327) 18:07:17.3	29.333°	34.749°	20	5.2	199`/77°/7°
96-145	1996 May 25 (145) 06:35:58.7	27.847°	53.594°	5	4.9	107°,/22°/88°

observed dispersion curves show great differences between the Shield and Platform paths, with the Shield being about 10 per cent faster. These variations in group velocity are similar to those obtained by Mokhtar & Al-Saeed (1994), McNamara *et al.* (1997), Mokhtar *et al.* (1997), Ritzwoller & Levshin (1998) and Pasyanos *et al.* (1998).

Estimates of the velocity structure of the two regions resulted from modelling the observed group velocity dispersion with a grid search scheme. We generated a wide range of models, and the Love and Rayleigh wave group velocity dispersion was computed for each model. The calculation of surface wave dispersion is very fast-much faster than that for a complete synthetic seismogram computed with the reflectivity method. We evaluated the performance of each model by computing the combined Love and Rayleigh wave group velocity misfit using the L2-norm.

We chose to fit the band 15-45 s because this period range is most sensitive to the structure of the crust and uppermost mantle. At periods shorter than 15 s the group velocity measurements can be biased by low-amplitude signals and scattered energy. The sediment thickness and upper crustal velocities control the short-period group velocities. Generally, the shape of the group velocity curve is controlled by the crustal thickness and velocity gradient. The velocity structure of the uppermost mantle, which controls the long-period behaviour, was estimated by fitting the body-wave phase arrivals, *Pn* and Sn, by waveform modelling (see next section).

Independent constraints on lithospheric velocity structure helped to fit the observed group velocities and waveforms. We used models of sediment thickness and crustal thickness for the Arabian Peninsula (Cornell University Middle East North Africa Project; Seber *et al.* 1997). These models are based on a large set of drill data, seismic reflection/refraction and gravity surveys. The sediment thickness is better constrained than crustal thickness. Deep sediments are present in the Arabian Gulf, but they gradually thin towards the Arabian interior. The crust is predicted to be 30-35 km near the Gulf of Aqaba and Red Sea and thickens to 40-45 km in central Arabia. Profiles generated through the Cornell models for the paths shown in Fig. 1 provided averages of sediment and crustal thickness. The Platform paths are characterized by average sediment and crustal thicknesses of 4 and 40 km, respectively. The average sediment thickness for the Arabian Shield paths is very low (< 1 km). Crustal thickness profiles for the Aqaba to Saudi paths are more variable (mean Moho depth of 32 km for the path to SODA and 42 km for the path to RAYN). Analysis of refraction data indicates the presence of a mid-crustal discontinuity in the Shield at about 20 km depth (Gettings *et al.* 1986). The sub-Moho P-wave velocity in the vicinity of the broadband stations is estimated to be 8.1 km s^{-1} (Gettings *et al.* 1986; Mellors *et al.* 1998). We fixed the sediment thickness (as stated above), the thickness of the lower crustal layer (20 km) and sub-Moho P- and S-wave velocities (8.10 and 4.55 km s^{-1}, respectively) for the group velocity modelling grid search. The P- to S-wave velocity scaling was determined by setting Poisson's ratio to 0.25 in the crust and 0.27 in the mantle (Christensen & Mooney 1995).

Three parameters were varied in the group velocity grid search: crustal thickness and the velocities of an upper and lower crustal layer. Given the above-stated constraints, we generated models which spanned a broad range of the parameter space and evaluated the performance of each model. Crustal thickness varied from 34 to 48 km, with an increment of 2 km; upper crustal P-wave velocity varied from 5.8 to 6.5 km s^{-1} with an increment of 0.1 km s^{-1}; and the lower crustal P-wave velocity varied from 6.2 to 7.2 km s^{-1} with an increment on 0.1 km s^{-1}. The range of models (704 in total) along with the 10 best-fitting models are shown in Fig. 3 for the Zagros-AFIF path. Notice that the 10 best-fitting models have similar velocities in the upper crustal layer (6.2-6.3), and that there is a trade-off between lower crustal velocity and crustal thickness to maintain a roughly constant vertical traveltime in the crust. The fits of the 10 best models to the group velocities observed at AFIF are also shown in Fig. 4. These models have remarkably similar dispersion curves and fit the data nearly equally well. A key result from Figs 3 and 4 is that the group velocities can constrain the velocities of the upper crust, but cannot simultaneously resolve the velocity of the lower crust and the crustal thickness.

Fig. 2 shows the observed and predicted group velocity curves for the best-fitting models that resulted from both group velocity and waveform modelling (described below). The group velocity curves are well fit; however, the large measurement uncertainties and the results of Figs 3 and 4 suggest that the observed curves can be fit by a wide variety of models.

WAVEFORM MODELLING

We modelled the observed waveforms to estimate the average 1-D seismic velocity structure of the Arabian Shield and Platform. The goal of this procedure is to determine a velocity model which predicts the arrival times and amplitudes of the main regional body wave phases *(Pn, Pnl* and *Sn)* and the Love and Rayleigh surface waves. Matching the observed waveforms with complete synthetic seismograms provides a more robust estimate of the structure than matching the

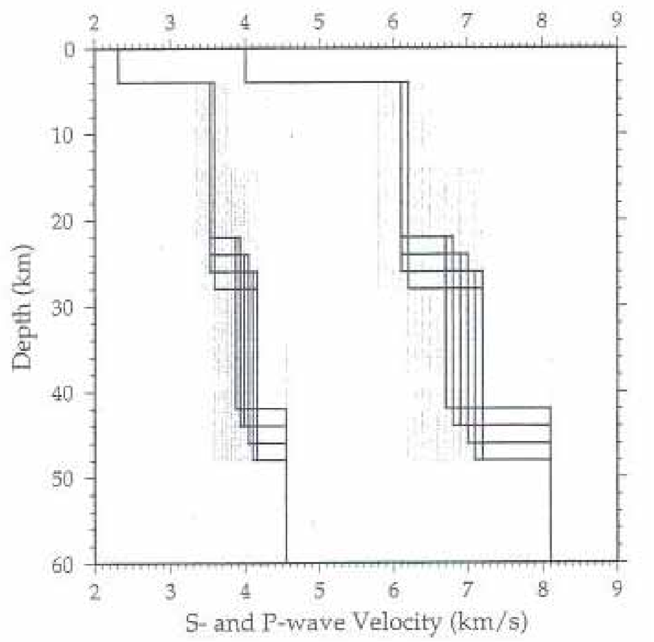

Figure 3. The *S*- and *P*-wave velocity models used in the group velocity grid search for the Zagros–AFIF path (grey lines). Values of the model parameters are given in the text. Also shown are the 10 best-fitting models (black lines).

Table 2. Arabian Shield and Platform lithospheric velocity models.

Arabian Shield Model thickness (km)	v_P (km s^{-1})	v_s (km s^{-1})	Arabian Platform Model thickness (km)	v_P (km s^{-1})	v_s (km s^{-1})
1	4.0	2.31	4	4.0	2.31
15	6.2	3.58	16	6.2	3.64
20	6.8	3.93	20	6.4	3.70
∞	7.9	4.30	∞	8.1	4.55

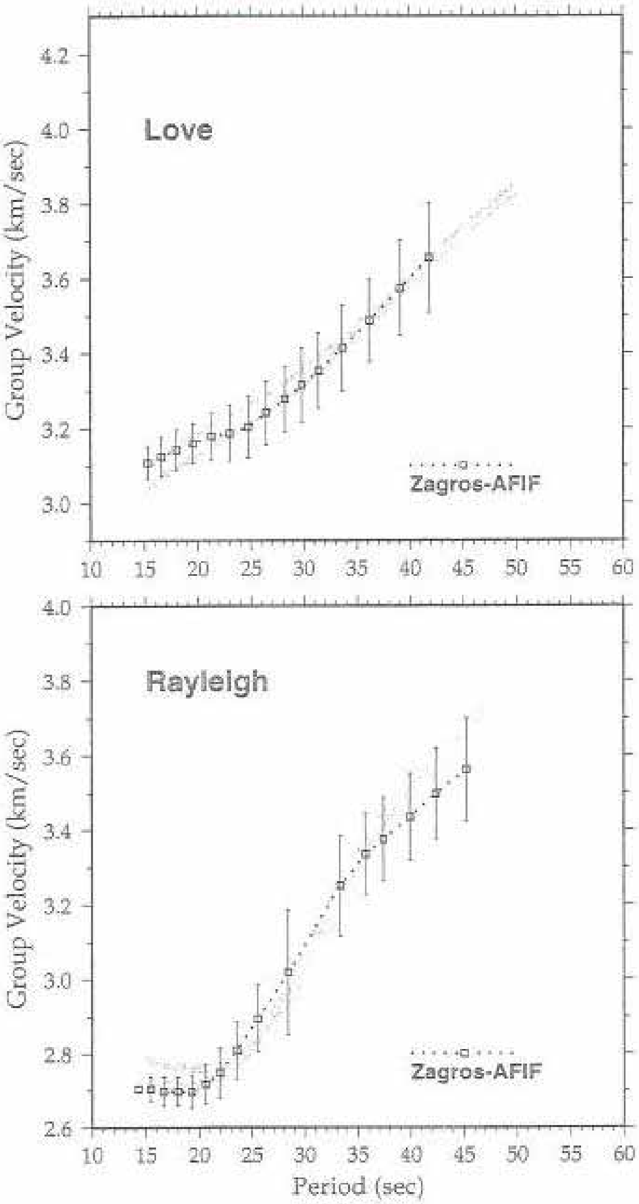

Figure 4. Observed group velocities for the Zagros–AFIF path (squares with error bars) and the fits of the 10 best models shown in Fig. 3.

observed group velocity dispersion alone. This is because the waveforms contain both the surface wave group and phase velocity information as well as the body wave arrivals and relative amplitudes of body-to-surface waves.

Waveforms were fit using a grid search scheme similar to that used in previous studies (e.g. Rodgers & Schwartz 1998). Synthetic seismograms were calculated for many velocity structures using the reflectivity method (Randall 1994). We expedited the waveform fitting process by limiting the grid search to those models that roughly fit the group velocity dispersion within the measurement uncertainties. The sediment thickness, lower crustal thickness and sub-Moho velocities were held constant in the waveform modelling grid search, similar to the group velocity modelling. We set shear wave attenuation in the crust to values consistent with those reported by Seber & Mitchell (1992): $Q_S=80$ in the sediment layer and upper crust, and $Q_S=150$ elsewhere. We set compressional wave attenuation to 9/5 times the shear wave attenuation. Consistent with Seber & Mitchell (1992), we found that crustal attenuation does not strongly affect the observed amplitudes for periods greater than about 10 s. Fig. 5 shows the velocity models used in the waveform modelling grid search for the Zagros–Saudi path. In these models, crustal thickness varied from 38 to 44 km, with an increment of 2 km; upper crustal *P*-wave velocity varied from 6.0 to 6.4 km s^{-1} with an increment of 0.1 km s^{-1}; and the lower crustal *P*-wave velocity varied from 6.2 to 6.8 km s^{-1} with an increment of 0.1 km s^{-1}.

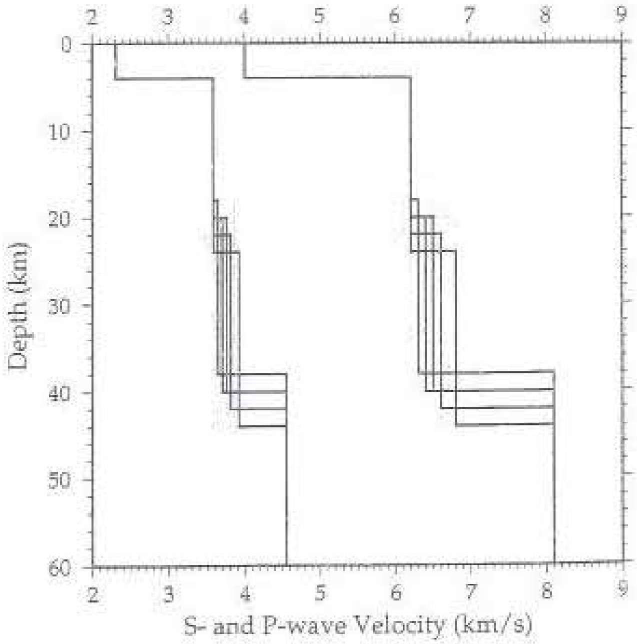

Figure 5. The *S*- and *P*-wave velocity models used in the waveform modelling grid search for the Zagros–AFIF path (grey lines). Values of the model parameters are given in the text. Also shown are the five best-fitting models (black lines).

These parameter values resulted in 140 models. We measured model performance with the combined three-component L2-norm misfit. The five best-fitting models are also shown in Fig. 5. Note the trade-off between the lower crustal velocity and crustal thickness, similar to in the group velocity modelling grid search (Fig. 3). However, the upper crustal velocity estimated from waveform modelling is very close to that estimated from group velocity modelling.

The model for the Shield paths obtained from waveform modelling is shown in Fig. 6 and Table 2, and the fits to the three-component waveforms recorded at AFIF are shown in Fig. 7(a). Because of weak long-period Rayleigh wave excitation, we included short periods down to 10 s. The Love and Rayleigh waves are well fit by the Arabian Shield model. The crustal thickness is 36 km, and average *P*- and *S*-wave crustal velocities are 6.42 and 3.70 km s^{-1}, respectively. However, the body-wave phases *Pn* and *Sn* on the vertical and radial components are not particularly well fit. In order to fit the relative timing of these arrivals, we had to decrease the sub-Moho *P*- and *S*-wave velocities to 7.9 and 4.30 km s^{-1}, respectively, corresponding to a high upper mantle Poisson's ratio of 0.29. These portions of the waveform could be poorly fit due to either focal mechanism errors (*Sn* is near nodal), attenuation, or crustal thickness variations along the path. It is well established from refraction and receiver function analysis that the crust is about 40 km thick and relatively fast beneath the temporary stations (Gettings *et al.* 1986; Sandvol *et al.* 1997). The Cornell crustal model (Seber *et al.* 1997) indicates that the crust is 30–35 km thick in the Gulf of Aqaba. Variations in the crustal thickness at the source and receiver will affect the body waves and surface waves differently. We chose to fit the surface waves, and we attribute the poor fit to the body waves as a possible focal mechanism and/or propagation effect due to non-plane layered structure.

The observed three-component component seismograms and synthetics for the best-fitting velocity model for the Arabian Platform (Zagros–Saudi paths) are shown in Fig. 7(b). Data and synthetics were filtered 20–100 s. The body wave and surface waves are generally well fit by the synthetics. Note that long-period noise affects the radial component near the *Pnl* arrival; however, the vertical component is relatively noise-free. The Platform model is shown in Fig. 6. The best-fitting model has a crustal thickness of 40 km, and crustal velocities are relatively slow (average *P*- and *S*-wave velocities of 6.07 and 3.50 km s^{-1}, respectively). The mantle velocities are typical of stable continental regions (*P*- and *S*-wave velocities of 8.10 and 4.55 km s^{-1}, respectively), with a normal mantle Poisson's ratio of 0.27 (Christensen & Mooney 1995).

Fig. 2 shows the fit of the group velocities predicted by the models estimated from waveform modelling to the observed group velocities. It is important to note that models that provide good fits to the observed waveforms predict the group

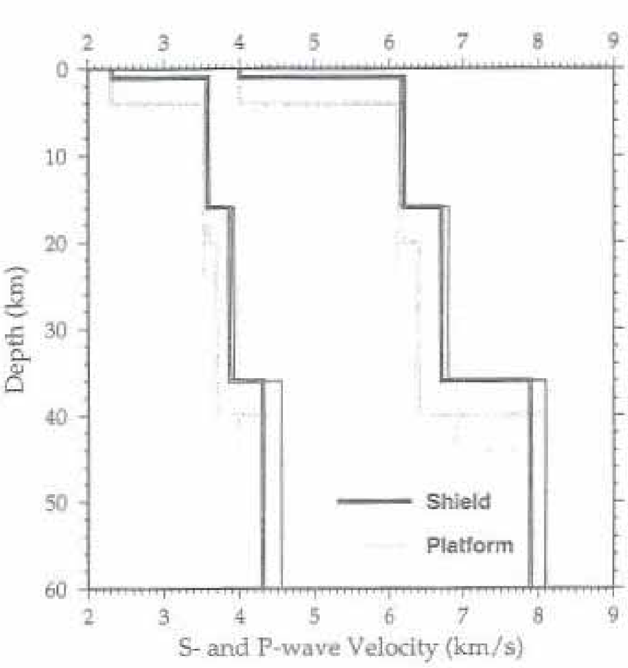

Figure 6. The Arabian Shield (black) and Platform (grey) velocity models. The thick lines are the preferred models, which provide the best fit to the waveforms. The thin lines are the models that provide the best fits to the group velocities.

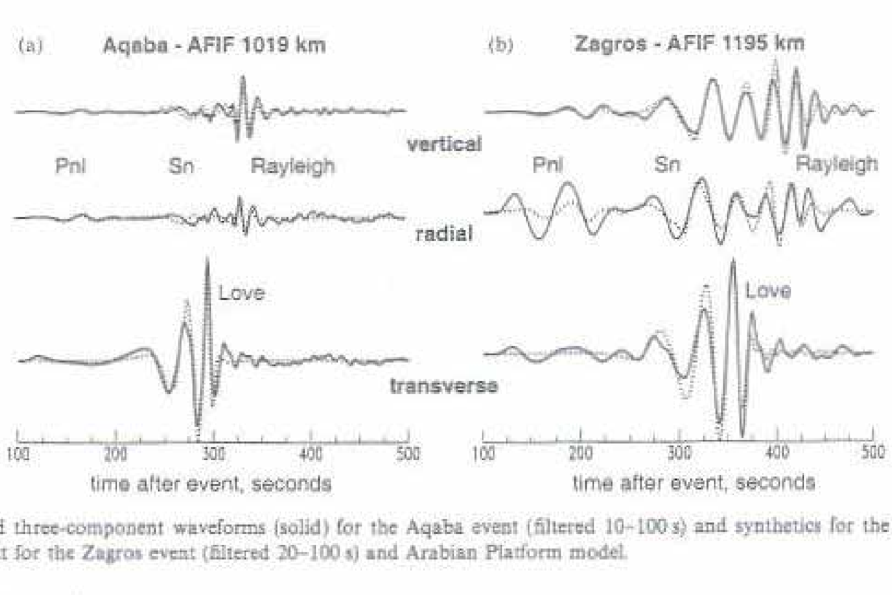

Figure 7. (a) Observed three-component waveforms (solid) for the Aqaba event (filtered 10–100 s) and synthetics for the Arabian Shield model (dashed). (b) As (a), but for the Zagros event (filtered 20–100 s) and Arabian Platform model.

C 1999 RAS, GJ1 138, 871-878

velocity dispersion within the uncertainty estimates. However, the models which gave the best fits to the observed group velocity dispersion do not necessarily fit the observed waveforms as well. Synthetics for these models misfit the surface wave phase, suggesting that modelling both group and phase velocities simultaneously will result in better fits to the waveforms. The crustal thickness and crustal velocities inferred from group velocity and waveform modelling are remarkably close for the Shield paths, but less so for the Platform path. This indicates that the group velocities provide valuable constraints on initial models and can be used to expedite the waveform fitting process. Especially encouraging is the agreement between the upper crustal velocities estimated from group velocity and waveform modelling. Because the group velocity calculation is roughly 20 times faster than the synthetic seismogram calculation, the benefit of time saved by constraining the waveform modelling parameter space with the results of group velocity modelling is substantial. The computational time saved can be spent investigating more detailed crustal structure (e.g. sediment layer structure, crustal velocity gradients) with waveform modelling.

DISCUSSION: LITHOSPHERIC COMPOSITION AND TECTONIC IMPLICATIONS

The velocity structures inferred from the above analysis require significantly different lithospheric compositions which must have resulted from different tectonic evolutions, The main differences between the crustal velocity profiles of the two regions (Fig. 6) are the excess sediments, the absence of a high-velocity lower crust, and the thicker crust in the Arabian Platform. These differences in velocity structure cannot be explained by a single crustal structure overlain with additional sediment on the Arabian Platform. Low crustal velocities in the Platform indicate a primarily felsic composition, while the faster velocities of the Shield indicate a m.afic lower crust (Christensen & Mooney 1995). Felsic composition of the Platform is consistent with orogenesis of this former active margin in late Proterozoic times (Stoeser & Camp 1985). It is interesting to note that the waveforms are best fit by a relatively uniform crust, whereas the group velocities prefer a velocity increase with depth. It is possible that our preferred Platform model is simple because we are fitting the longer-period (20 s and higher) surface waves. An important difference between waveform modelling and group velocity modelling is that group velocities are modelled with all frequencies being weighted equally; however, waveforms have some frequencies more strongly represented than others due to source excitation and propagation effects. For example, a 20-s Rayleigh wave (the Airy phase} is typically the largest-amplitude surface wave for continental paths. When the waveform misfit is measured by the L2-norm, the Airy phase will dominate the sensitivity of the data to the structure at the expense of the smalleramplitude body waves or long-period surface waves. When periods as short as 10 s were included, we estimated a similar model. Regardless of which period band was used to estimate the velocity structure, the average crustal velocities for the Platform paths are low and there is no suggestion of a strong velocity gradient.

Average crustal velocities for our Arabian Shield model are slightly slower than those from previous, more localized studies (e.g. Gettings *et al.* 1986; Sandvol *et al.* 1998; Al-Amri 1998). This may arise due to slower along-path velocities near the Gulf of Aqaba or beneath the volcanic centres. The Shield model includes a strong velocity increase between the upper and lower crust. The high velocities in the lower crust of the Arabian Shield suggest a mafic composition at depth. This is consistent with the island arc origin of the westernmost terranes of the Shield. The presence of volcanics on the Arabian Shield may have resulted in mafic addition to the crust, which would increase bulk crustal velocities. A bulk mafic composition would result in a higher than average crustal Poisson's ratio (>0.27). Unfortunately, the *Pnl* wave is poorly excited for the Aqaba event, preventing us from obtaining a good estimate of the crustal P-wave velocity for this path. The observation that the crustal velocities are rather fast and that short-period L_g waves are not strongly attenuated suggests that partial melt associated with volcanism is not wide-spread throughout the crust in western Arabia. However, from the paths used in this study we cannot determine the lateral extent of any anomalous zone. The low sub-Moho velocities, high Poisson's ratio (0.29) in the shallow mantle, the absence of efficient short-period *Sn* in the Arabian Shield (Mellors *et al.* 1998) and the presence of volcanic centres are all consistent with the presence of partially molten mantle directly beneath the Moho.

Finally, the inferred seismic velocity structures have implications for the mass balance of the Arabian Peninsula. The Arabian Shield is topographically higher on average than the Arabian Platform, yet the crust is thinner beneath the Shield. Furthermore, the inferred crustal velocities imply that the Shield crust is denser than the Platform. The higher topography of the Shield could be supported in part by less dense, low-velocity mantle. While we cannot directly infer dynamical properties of the Arabian Shield, our results are broadly consistent with hot, upwelling asthenosphere as reported by Camp & Roobol (1992) based on analysis of volcanic rocks. Future investigations using broadband seismic data from a dense network will provide further insights into the structure of this complex region.

ACKNOWLEDGMENTS

This study would not have been possible without the data collection and organizational efforts of Frank Vernon and colleagues from the University of California, San Diego. Group velocity dispersion was measured using programs written by Charles Ammon of Saint Louis University. Models of basalt cover, sediment and crustal thickness were provided by Eric Sandvol, Dogan Seber and Muawia Barazangi of Cornell University. Comments by Victor Camp and Steve Myers are gratefully acknowledged. Careful reviews by Eric Sandvol and Mark Gettings and editorial assistance from Steve Ward improved the original manuscript. This work was performed in part under the auspices of the US Department or Energy by the Lawrence Livermore National Laboratory under contract W-7405-ENG-48. This is LLNL contribution UCRL-JC-132098. This is contribution number 388 of the W. M. Keck Seismological Laboratory and the Institute ei Tectonics, University of California, Santa Cruz.

REFERENCES

Al-Amri, A.M.S., 1998. The crustal structure of the western Arabian platform from the spectral analysis of long-period P-wave amplitude ratios, *Tectonophysics, 290,* 271-283.

Al-Amri, A.M.S., 1999. The crustal and upper-mantle structure of the interior Arabian platform, *Geophys. J. Int., 136,* 421-430.

Camp, V. & Roobol, M., 1992. Upwelling asthenosphere beneath western Arabia and its regional implications, *J. geophys. Res., 97,* 15 255-15 271.

Christensen, N. & Mooney, W., 1995. Seismic velocity structure and composition of the continental crust: a global view, *J. geophys. Res.,* 100, 9761-9788.

Gettings, M., Blank, H., Mooney, W. & Healey, J., 1986. Crustal structure of southwestern Saudi Arabia, *J. geophys. Res., 91,* 6491-6512.

McNamara, D., Hazier, S. & Walter, W., 1997. Velocity structure across northern Africa, southern Europe, the Middle East and the Arabian Peninsula from surface wave dispersion, EOS, *Trans. Am. geophys. Un., 78,* F499.

Mellors, R., Vernon, F., Camp, V., Al-Amri, A., Gharib, A. & AI-Dial, M., 1998. Regional waveform propagation in the Saudi Arabian Peninsula, in press.

Mokhtar, T. & Al-Saeed, M., 1994. Shear wave velocity structures of the Arabian Peninsula, *Tecronophysics, 230,* 105-125.

Mokhtar, T., Ammon, C., Ghalib, H. & Herrmann, R., 1997. Lithospheric structure beneath Arabia, EOS, *Trans. Am. geophys. Un., 78,* F499.

Pasyanos, M., Walter, W., Hazler, S. & McNamara, D., 1998. Surface wave research in the Middle East and North Africa, in *Proc. 20th Ann. Seismic Research Symp. on Monitoring a Comprehensive Test Ban Treaty, pp.* 476-485, eds Fontroy, J., Heatley, D., Warren, J., Chavez, F. & Meade, C., Dept of Defense, Nuclear Treaty Programs, Washington.

Randall, G., 1994. Efficient calculation of complete differential seismograms for laterally homogeneous earth models, *Geophys. J. Int.,* 118, 245-254.

Ritzwoller, M. & Levshin, A., 1998. Eurasian surface wave tomography: Group velocities, *J. geophys. Res., 103,* 4839-4878.

Rodgers, A. & Schwartz, S., 1998. Lithospheric structure of the Qiangtang Terrane, northern Tibetan Plateau, from complete regional waveform modeling: evidence for partial melt, *J. geophys. Res., 103,* 7137-7152.

Sandvol, E., Seber, D., Barazangi, M., Vernon, F., Mellors, R. & Al-Amri, A., 1998. Lithospheric velocity discontinuities beneath the Arabian Shield, *Geophys. Res. Lett., 25,* 2873-2876.

Seber, D. & Mitchell, B., 1992. Attenuation of surface waves across the Arabian Peninsula, *Tectonophysics, 204,* 137-150.

Seber, D., Vallve, M., Sandvol, E., Steer, D. & Barazangi, M., 1997. Middle East tectonics: applications of geographical information Systems (GIS), *GSA Today, 7, 1-5.*

Stoeser, D. & Camp, V., 1985. Pan-African microplate accretion of the Arabian shield, *Geol. Soc. Am. Bull.,* 96, 817-826.

Walter, W. & McNamara, D., 1997. Propagation characteristics of Lg throughout the Middle East, Mediterranean, southern Europe and northern Africa, EOS, *Trans. Am. geophys. Un., 78,* F499.